J. Fluid Mech. (1987), *vol.* 176, *pp.* 379–402
Printed in Great Britain

Theory of dynamic permeability and tortuosity in fluid-saturated porous media

By DAVID LINTON JOHNSON, JOEL KOPLIK AND ROGER DASHEN†

Schlumberger–Doll Research, Old Quarry Road, Ridgefield, CT 06877-4108, USA

We consider the response of a Newtonian fluid, saturating the pore space of a rigid isotropic porous medium, subjected to an infinitesimal oscillatory pressure gradient across the sample. We derive the analytic properties of the linear response function as well as the high- and low-frequency limits. In so doing we present a new and well-defined parameter Λ, which enters the high-frequency limit, characteristic of dynamically connected pore sizes. Using these results we construct a simple model for the response in terms of the exact high- and low-frequency parameters; the model is very successful when compared with direct numerical simulations on large lattices with randomly varying tube radii. We demonstrate the relevance of these results to the acoustic properties of non-rigid porous media, and we show how the dynamic permeability/tortuosity can be measured using superfluid ^{4}He as the pore fluid. We derive the expected response in the case that the internal walls of the pore space are fractal in character.

1. Introduction

The elastodynamic properties of porous media are interesting in part because of the possibility of macroscopic relative motion between the fluid and the solid constituents. These effects are of prime importance in understanding fourth sound in a superfluid/superleak system (Johnson 1980), pressure diffusion through porous media (Chandler & Johnson 1981; Chandler 1981), slow waves and the consolidation transition (Johnson & Plona 1982), elastodynamics of gels (Johnson 1982) as well as the acoustic properties of 'ordinary' porous media saturated with 'ordinary' fluids (Johnson *et al.* 1982). These properties are discussed in a review of recent work (Johnson 1984). One of the ingredients of the theory of these phenomena, as well as being an interesting effect in its own right, is the response of a simple fluid entrained in a rigid porous medium and subjected to a harmonic pressure drop across the sample; this article is devoted to an understanding of that response, which has been the subject of other recent work (Attenborough 1983; Auriault, Borne & Chambon 1985; Bedford, Costley & Stern 1984).

In §2 we pose the problem and we show that the relevant response functions, the dynamic permeability or dynamic tortuosity, are analytic functions of frequency except for singularities on the negative imaginary axis. We also derive the rigorous results for the high- and low-frequency behaviour; the distinction between high and low frequencies is whether the viscous skin depth, $\delta = (2\eta/\rho_f \omega)^{\frac{1}{2}}$, is small or large compared to the sizes of the pores. These results are used in §3 to construct a simple model of the response for arbitrary frequency; the parameters in this theory are those appropriate to the high- and low-frequency behaviour. As a test of the model we compare it with numerical simulations on large lattices constructed by randomly

† Also at Institute for Advanced Study, Princeton, NJ 08540, USA.

distributing tubes of random radii on the bonds thereof. In §4 we demonstrate the relevance of our results to cases in which the solid is deformable. We demonstrate the power of superfluid ^{4}He acoustics as a probe of this dynamic response function in §5. Section 6 is devoted to dynamic permeability in a porous medium whose internal surface is a fractal.

2. Definitions and general properties

Consider a homogeneous, isotropic, porous solid with porosity (pore volume fraction) ϕ. We suppose that the solid is not deformable, either because it has a very large density, or very large elastic modulii, or both. This solid is saturated with an incompressible Newtonian fluid of density ρ_f and viscosity η. In practice, the results we shall obtain will apply to acoustics as long as the wavelength of sound (in the fluid) is much larger than the characteristic sizes of pores and grains in the medium, ensuring that the fluid may be considered to be incompressible on the scale of the pore sizes. We assume that the properties of the fluid are unaffected by its proximity to the walls of the solid. We also assume that the fluid has a negligible thermal expansion coefficient on any scale; this assumption ensures that pressure–density variations are decoupled from temperature variations (Landau & Lifshitz 1959).

The porous medium occupies the space $0 < x < L$, where L is extremely large compared to the sizes of the pores. The transverse (y, z) size of the system does not enter into the following, and may be taken as infinite, or as periodic, or as impermeable with finite extent. We apply a macroscopic pressure gradient, $\nabla P e^{-i\omega t}$, to the sample and follow the linear (i.e. small amplitude) response of the fluid to this applied gradient. The response is most conveniently defined in terms of the macroscopically averaged fluid velocity $\boldsymbol{v}(\omega)$, which is defined so that $\phi \boldsymbol{v} \cdot \hat{\boldsymbol{n}} A$ is the amount of fluid crossing a macroscopic surface of area A having an outward normal $\hat{\boldsymbol{n}}$; since the area fraction actually in contact with fluid is ϕ, $\boldsymbol{v}$ represents a macroscopic fluid velocity. Under the stated assumptions $\boldsymbol{v}$ is obviously linearly related to the pressure gradient at any frequency

$$\tilde{\alpha}(\omega)\rho_f \frac{\partial \boldsymbol{v}}{\partial t} = -\nabla P, \quad \phi \boldsymbol{v} = -\frac{\tilde{k}(\omega)}{\eta}\nabla P. \tag{2.1a,b}$$

The frequency-dependent tortuosity $\tilde{\alpha}(\omega)$ is defined in (2.1a) by analogy with the response of an ideal (non-viscous) fluid for which $\tilde{\alpha}$ is real-valued and frequency independent (Johnson & Sen 1981); it is a dimensionless quantity. The frequency-dependent permeability $\tilde{k}(\omega)$ is defined in (2.1b) by analogy with the steady-state ($\omega = 0$) definition (Scheidegger 1974). it has the dimensions of area (the conventional oil-field unit is the darcy: 1 darcy $\approx 10^{-8}$ cm^2). Obviously, the two quantities are related to each other:

$$\tilde{\alpha}(\omega) = \frac{i\eta\phi}{\tilde{k}(\omega)\omega\rho_f}. \tag{2.1c}$$

The relationship between $\tilde{\alpha}(\omega)$ and $\tilde{k}(\omega)$ is roughly analogous to that between the dynamic electrical conductivity $\tilde{\sigma}(\omega)$ and the dynamic dielectric function $\tilde{\epsilon}(\omega)$ which arise in the electrodynamics of continuous media (Pines 1964, p. 123): $\tilde{\epsilon}(\omega) = 1 + 4\pi i\tilde{\sigma}(\omega)/\omega$.

We shall be using the results of this article to predict the properties of the plane-wave normal modes when the fluid has a finite compressibility; our results are valid only for frequencies such that the wavelength is so large that the fluid is still to be considered incompressible on a microscopic scale. This is analogous to the use

of a long-wavelength dielectric function $\tilde{\epsilon}(\omega)$ to calculate the dispersion relation of electromagnetic modes in a material. In order to calculate the dispersion relations we need the continuity equation

$$\nabla\cdot(\rho_f\phi\boldsymbol{v})+\frac{\partial}{\partial t}(\phi\rho_f)=0, \tag{2.2}$$

and the constitutive equation

$$\frac{\delta\rho_f}{\rho_f}=\frac{\delta P}{K_f}, \tag{2.3}$$

where K_f is the bulk modulus of the fluid. If we look for plane-wave solutions, varying as $e^{i(q\cdot r-\omega t)}$ to the linearized versions of (2.1)–(2.3), we find dispersion relations which can be stated either as

$$q(\omega)=(\tilde{\alpha}(\omega))^{\frac{1}{2}}\frac{\omega}{V_f}, \tag{2.4a}$$

where $V_f=(K_f/\rho_f)^{\frac{1}{2}}$ is the speed of sound in the fluid, or as

$$q(\omega)=\left(\frac{i\omega}{\tilde{C}(\omega)}\right)^{\frac{1}{2}}, \tag{2.4b}$$

where $\tilde{C}(\omega)=\tilde{k}(\omega)K_f/\eta\phi$. Thus, if one is in a frequency range where $\tilde{\alpha}(\omega)$ is essentially real-valued and independent of frequency, the mode propagates non-dispersively with phase velocity $V_f/\tilde{\alpha}^{\frac{1}{2}}$, as has been noted previously (Johnson 1980; Johnson & Plona 1982). If, on the other hand, one is in a frequency range where $\tilde{k}(\omega)$ is essentially real-valued and independent of frequency, then the normal-mode coordinates follow a diffusion equation with a diffusivity $\tilde{C}$, as has also been noted previously (Chandler & Johnson 1981; Johnson & Plona 1982). Inasmuch as both possibilities do occur (see below), it is convenient to analyse the response of the system in terms of $\tilde{\alpha}(\omega)$ and $\tilde{k}(\omega)$ simultaneously.

We wish now to consider properties of $\tilde{\alpha}(\omega)$, $\tilde{k}(\omega)$ when ω is extended to complex values. We note that $\tilde{k}(\omega)$ describes the response of the system to an applied stimulus. The causality requirement (Landau & Lifshitz 1960, p. 257), that the system does not respond until after the stimulus is applied, automatically guarantees that $\tilde{k}(\omega)$ is an analytic function for all ω in the upper half-plane; $\tilde{k}(\omega)$ has no branch points or poles if $\mathrm{Im}\,(\omega)>0$. Therefore, $\tilde{\alpha}(\omega)$ has no zeros in the upper half-plane. Similarly, $\tilde{\alpha}(\omega)$ is also a causal response function because it describes the induced pressure gradient as a response to an imposed fluid flow on the sample; both $\tilde{\alpha}(\omega)$ and $\tilde{k}(\omega)$ have no poles, branch points, or zeros in the upper half-ω-plane. (The analogous situation in electrodynamics is that both the conductivity and the resistivity are causal response functions, depending on whether the system is subjected to a voltage source or a current source, respectively.) Any singularities in $\tilde{\alpha}(\omega)$ or $\tilde{k}(\omega)$ must occur in the lower half-plane; in Appendix A we show that, for the particular case at hand, the only singularities occur on the negative imaginary axis. We note that, as an artifact of the way it is defined, $\tilde{\alpha}(\omega)$ has a simple pole at $\omega=0$; we shall explicitly assume that there are no other singularities in either $\tilde{\alpha}(\omega)$ or $\tilde{k}(\omega)$ at $\omega=0$.

We have the further requirement that if a real-valued stimulus, $\nabla P e^{-i\omega t}+\nabla P^* e^{+i\omega^* t}$, is applied, then the response is also real-valued; this guarantees a symmetry in the response functions across the imaginary axis (Landau & Lifshitz 1960, p. 257)

$$\tilde{\alpha}(-\omega^*)=\tilde{\alpha}^*(\omega),\quad \tilde{k}(-\omega^*)=\tilde{k}^*(\omega), \tag{2.5a,b}$$

where the asterisk signifies complex-conjugation.

We now consider the limiting cases of low- and high-frequency response. Obviously, for low enough frequencies the dynamic permeability approaches its d.c. value:

$$\lim_{\omega\to 0} \tilde{k}(\omega) = k_0, \quad \lim_{\omega\to 0} \tilde{\alpha}(\omega) = \frac{i\eta\phi}{k_0\rho_f\omega}, \tag{2.6a,b}$$

where k_0 is the real-valued permeability conventionally measured in an experiment in which the sample is subjected to a static pressure drop. For fields which are slowly varying (in time), the pressure, flow rate, etc. follow a diffusion equation with a diffusivity $C = k_0 K_f/\eta\phi$.

In the limit of high frequencies, the viscous skin depth, $\delta = (2\eta/\rho_f\omega)^{\frac{1}{2}}$, eventually becomes much smaller than any characteristic pore size. From the microscopic Stokes equation (A 1), the vorticity, $\nabla\times\boldsymbol{u}$, obeys the diffusion equation with a diffusion length given by δ. This means that any vorticity generated at the pore walls decays to zero as one moves away from the wall into the bulk of the pore (Landau & Lifshitz 1959, p. 91). Therefore, except for a boundary layer of thickness δ, the fluid motion is given by potential flow, $\boldsymbol{u}_p = -\nabla\psi$, for some ψ. Thus, the flow pattern is identical with that for an ideal fluid, except in the boundary layer. For an ideal fluid the quantity $\tilde{\alpha}$ is a real-valued quantity α_∞, independent of fluid properties (Johnson & Sen 1981). This suggests that

$$\lim_{\omega\to\infty} \tilde{\alpha}(\omega) = \alpha_\infty + C(-i\omega)^{-p}, \tag{2.7}$$

for some $p > 0$; we shall verify this form (below) and show that $p = \frac{1}{2}$. Because of the reflection symmetry (2.5) both α_∞ and C are real-valued.

The significance of this result is that, from (2.4a) and the discussion following it, the mode is a propagatory one with phase speed $V = V_f/(\alpha_\infty)^{\frac{1}{2}}$. α_∞ is conveniently measured using superfluid ^{4}He as the pore fluid; it is related to the 'index of refraction of the porous medium' by $\alpha_\infty = n^2$ (Johnson *et al.* 1982, and references therein).

We also have the result that α_∞ is related to the electrical conductivity of the porous medium. Assuming that the porous solid is insulating, the electrical conductivity σ is proportional to the electrical conductivity of the pore fluid σ_f by $\sigma = \sigma_f/F$, where F is a geometrical factor. It is a rigorous result (Brown 1980), apparently known to Lord Rayleigh, that

$$\alpha_\infty = F\phi. \tag{2.8}$$

One can, therefore, experimentally measure this high-frequency acoustics parameter by non-acoustical techniques. The equivalence of these two different ways of measuring α_∞ has been verified experimentally in a series of fused glass-bead samples (Johnson *et al.* 1982).

In fact, an exact expression exists relating α_∞ to the microscopic potential-flow solution, $\boldsymbol{u}_p(\boldsymbol{r})$:

$$\alpha_\infty = \frac{\phi A|\psi_L|^2}{L\int|\boldsymbol{u}_p(\boldsymbol{r})|^2\,dV}, \tag{2.9}$$

where the integration is over the pore space within a slab of material of thickness L and lateral area A, and $\boldsymbol{u}_p(\boldsymbol{r}) = -\nabla\psi$ is determined by the solution of the mathematical problem $\nabla^2\psi = 0$, subject to the boundary conditions $\psi(x=0) = 0$, $\psi(x=L) = \psi_L$ (a constant), and $\hat{\boldsymbol{n}}\cdot\nabla\psi = 0$ at the pore walls. Equation (2.9) can be established most simply by considering a related problem, the electrical conductivity of an inhomogeneous material having a local conductivity $\sigma(\boldsymbol{r})$ which vanishes in the

solid region and has a constant value σ_f in the pore space; $\tilde{\psi}(\boldsymbol{r})$ may be taken as the potential. We consider the identity

$$\nabla\cdot\{\psi^*\sigma\nabla\psi\} = \sigma(\boldsymbol{r})|\nabla\psi|^2 + \psi^*\nabla\cdot\{\sigma\nabla\psi\},$$

in which the second term on the right-hand side vanishes because of current conservation. If we then integrate this identity over a slab of material subjected to the applied voltage drop ψ_L, then by Gauss's theorem the left-hand side is simply $-\psi_L^* I$, where I is the total current. It is straightforward to solve for the macroscopic conductivity of the system from which (2.9) follows because of (2.8). Similar expressions have been derived by Bergman and collaborators (Bergman 1979; Bergman, Halperin & Hohenberg 1975), but (2.9) is most convenient for our purposes.

Furthermore, the corrections to the extreme high-frequency limit, the second term on the right-hand side of (2.7), can also be related, exactly, to the microscopic potential-flow field, $\boldsymbol{u}_p(\boldsymbol{r})$, by considering the attenuation of sound in two different but equivalent ways. The intensity of a sound wave decays exponentially, on a macroscopic scale, as $\exp(-2q''x)$, where q'' is the imaginary part of the wave vector; in this high-frequency limit, an expression for q'' can be determined by substituting (2.7) into (2.4a). On a microscopic scale, q'' can be related (Landau & Lifshitz 1959, p. 299) to the exact microscopic velocity field, $\boldsymbol{u}(\boldsymbol{r})$:

$$q'' = \frac{|\dot{E}_{\mathrm{mech}}|}{2S_0}. \tag{2.10}$$

S_0 is the energy flux density; it is equal to the speed of sound, $V_f/(\alpha_\infty)^{\frac{1}{2}}$, times the energy density:

$$S_0 = \frac{V_f}{(\alpha_\infty)^{\frac{1}{2}}}\tfrac{1}{2}\rho_f\frac{1}{LA}\int|\boldsymbol{u}_p(\boldsymbol{r})|^2\,\mathrm{d}V, \tag{2.11}$$

where the integration is over the pore space within a slab of material of thickness L and lateral area A. We have assumed a sinusoidal time dependence and averaged over a cycle. The rate of energy dissipation per unit volume $\dot{E}_{\mathrm{mech}}$ is

$$\dot{E}_{\mathrm{mech}} = -\tfrac{1}{4}\eta\frac{1}{LA}\int\left|\frac{\partial u_i}{\partial x_k}+\frac{\partial u_k}{\partial x_i}\right|^2\mathrm{d}V, \tag{2.12}$$

where we have explicitly assumed incompressibility of the fluid on the size scale of the pores (Landau & Lifshitz 1959, p. 299). As we have shown above, the fluid motion is that of potential flow, $\boldsymbol{u}\approx\boldsymbol{u}_p = -\nabla\psi$, except in a boundary layer of thickness δ at the pore walls, where the velocity goes to zero. We divide the integration in (2.12) into two parts, the bulk of the pore space and the boundary layer. The former gives a contribution to (2.12) which can be shown to be equal to an integral over the bounding surface of this region (Landau & Lifshitz 1959, p. 54):

$$\dot{E}^{(\mathrm{V})}_{\mathrm{mech}} = -\frac{\eta}{2LA}\int\nabla|\boldsymbol{u}_p(\boldsymbol{r})|^2\cdot\hat{\boldsymbol{n}}\,\mathrm{d}A, \tag{2.13}$$

which is independent of frequency; obviously a negligible error is introduced by extending the surface of integration in (2.13) to be that of the actual pore walls. To evaluate the contribution to (2.12) from the boundary region we note that since δ is arbitrarily small at high enough frequencies, the walls of the pores appear to be flat in the region where the velocity goes from zero at the wall to the value $\boldsymbol{u}_p$ in the pore region. Thus, the velocity field in this region is (Landau & Lifshitz 1959, p. 91)

$$\boldsymbol{u}(\boldsymbol{r}) = \boldsymbol{u}_p(\boldsymbol{r}_w)\,[1-\mathrm{e}^{\mathrm{i}K\beta}], \tag{2.14}$$

where β is a local coordinate measured from the pore wall at position $\boldsymbol{r}_w$ into the bulk of the pore and $K = (i\omega\rho_f/\eta)^{\frac{1}{2}} = (1+i)/\delta$ is the shear wave vector at frequency ω. Therefore, the contribution of this boundary region to (2.12) is evaluated by substituting (2.14) into (2.12):

$$\dot{E}^{(S)}_{\text{mech}} = -\frac{1}{2LA}(\tfrac{1}{2}\eta\rho_f\omega)^{\frac{1}{2}}\int |\boldsymbol{u}_p(\boldsymbol{r}_w)|^2\,dA, \tag{2.15}$$

where the integration is over the boundary walls of the pore space; (2.15) clearly dominates (2.13) at high frequencies. Combining (2.4a), (2.7), (2.10), (2.11), (2.12), and (2.15), we find that $p = \frac{1}{2}$ and we have an explicit expression for C. In fact (2.7) can be more clearly written as

$$\lim_{\omega\to\infty} \tilde{\alpha}(\omega) = \alpha_\infty\left[1+\left(\frac{i\eta}{\rho_f\omega}\right)^{\frac{1}{2}}\frac{2}{\Lambda}\right], \tag{2.16a}$$

$$\lim_{\omega\to\infty} \tilde{k}(\omega) = \frac{i\eta\phi}{\alpha_\infty\rho_f\omega}\left[1-\left(\frac{i\eta}{\rho_f\omega}\right)^{\frac{1}{2}}\frac{2}{\Lambda}\right], \tag{2.16b}$$

where the parameter Λ has the dimensions of length and is given by

$$\frac{2}{\Lambda} = \frac{\int |\boldsymbol{u}_p(\boldsymbol{r}_w)|^2\,dA}{\int |\boldsymbol{u}_p(\boldsymbol{r})|^2\,dV}. \tag{2.17}$$

The integration in the numerator of (2.17) is over the walls of the pore–grain interface; that of the denominator is over the pore volume. Thus $2/\Lambda$ is essentially the surface-to-pore-volume ratio of the pore–solid interface in which each area or volume element is weighted according to the local value of the field $\boldsymbol{u}_p$. (The motivation for defining Λ in this way will become apparent.) Equations (2.16) and (2.17) are exact, new results, applicable to any porous medium. Both α_∞ and Λ are independent of fluid properties and each is a characteristic parameter of the given porous medium; in principle, each is determined from the solution of the same mathematical problem, using (2.9) or (2.17).

We have already discussed how α_∞ is measured; Λ can be deduced from a measurement of the attenuation of a sound mode in the high-frequency limit. It is convenient to express the attenuation in terms of the specific attenuation in per cycle, $1/Q = 2q''/q'$, which is derived from (2.4a) and (2.16):

$$\lim_{\omega\to\infty}\frac{1}{Q} = \frac{\delta}{\Lambda}. \tag{2.18}$$

In fact, Λ has already been measured in a few samples of porous solids using superfluid ^{4}He, which we shall discuss in §5.

We conclude this section with a very simple example of an exactly solvable model which illustrates the general properties explicitly. The porous medium consists of fluid-saturated cylindrical tubes of radius R whose axes form an angle θ with the direction of the applied pressure gradient. The solution is given in different, but equivalent, forms by different authors (Bedford *et al.* 1984; Biot 1956a, b; Jayasinghe, Letelier & Leutheusser 1974; Zwikker & Kosten 1949). We need the volume flow rate $\dot{V}$ through a tube of length L having an imposed sinusoidally varying pressure drop ΔP:

$$\dot{V} = \frac{\pi R^2}{i\omega\rho_f}\left[\frac{2J_1(KR)}{KRJ_0(KR)}-1\right]\frac{\Delta P}{L}, \tag{2.19}$$

where the J_i are Bessel functions. This expression has been verified experimentally in U-tube oscillations (Jayasinghe *et al.* 1974). From (2.19) it is straightforward to deduce the dynamic permeability/tortuosity:

$$\tilde{\alpha}(\omega) = \left[\left(1 - \frac{2J_1(KR)}{KRJ_0(KR)}\right)\cos^2\theta\right]^{-1}, \tag{2.20a}$$

$$\tilde{k}(\omega) = \frac{\phi\eta}{i\omega\rho_f}\left[\frac{2J_1(KR)}{KRJ_0(KR)} - 1\right]\cos^2\theta. \tag{2.20b}$$

By inspection, $\tilde{\alpha}(\omega)$ and $\tilde{k}(\omega)$ have singularities only on the negative imaginary axis, and they obey the reflection symmetry (2.5); by considering the high- and low-frequency limits we can relate the general parameters to the specific:

$$\alpha_\infty = \frac{1}{\cos^2\theta}, \quad k_0 = \tfrac{1}{8}\phi R^2\cos^2\theta, \quad \Lambda = R. \tag{2.21a,b,c}$$

Equations (2.21*a*, *b*) are given in Scheidegger (1974); (2.21*c*) is obvious from the definition (2.17) because $\boldsymbol{u}_p(\boldsymbol{r})$ is constant in each tube. This was the motivation for defining Λ in the way that we did.

In general, the parameters α_∞, k_0, and Λ are unrelated and independently measurable, but if one can model the response of the system as a set of non-intersecting tubes canted at an effective angle θ, one may expect the parameters to be related to each other, at least approximately, by (2.21*a*–*c*):

$$\frac{8\alpha_\infty k_0}{\phi\Lambda^2} = 1. \tag{2.22}$$

(If the porous medium can be modelled as canted slabs of fluid, for which Λ is equal to the width of the slab, then the 8 in (2.22) is replaced by a 12.) A relationship equivalent to (2.22), or modified by the introduction of dimensionless factors, is implicit in all previous approaches to this problem. For example, in the notation of Biot (1956*a*, *b*) the left-hand side of (2.22) is equal to $\delta^2/8\xi$, where δ is the 'structural factor' and ξ is the 'sinuosity factor'. In the notation of Attenborough (1983), the left-hand side of (2.22) is equal to n^2/s where n is the 'dynamic shape factor' and s is the 'static shape factor'. If one makes reasonable guesses of the values of these dimensionless parameters, one is then able, in effect, to deduce values of Λ in terms of the other parameters ϕ, k_0, and α_∞. In the present article, we wish to emphasize that all parameters in (2.22) are independently measurable and thus its approximate validity can be directly tested (see §5).

3. Model for frequency dependence of dynamic permeability

In this section we develop a model, in terms of simple analytic functions, for the frequency dependence of $\tilde{\alpha}(\omega)$. We require that the model satisfies the general properties of §2 and that it depends only on the four parameters, α_∞, k_0, Λ, and ϕ which are well defined for any porous medium; we do not assume that these four are related to each other by (2.22). Let us consider $\tilde{\alpha}(\omega)$ in the form

$$\tilde{\alpha}(\omega) = \alpha_\infty + \frac{i\eta\phi}{\omega k_0\rho_f}F(\omega), \tag{3.1}$$

where, because of (2.6) and (2.16) respectively, $F(\omega)$ has the following properties:

$$F(0) = 1, \tag{3.2a}$$

$$\lim_{\omega\to\infty} F(\omega) = \frac{2k_0\alpha_\infty}{\Lambda\phi}\left[\frac{-i\omega\rho_f}{\eta}\right]^{\frac{1}{2}}, \tag{3.2b}$$

The simplest possible model for $F(\omega)$ is

$$F(\omega) = \left\{1 - i\frac{4\alpha_\infty^2 k_0^2 \rho_f \omega}{\eta\Lambda^2\phi^2}\right\}^{\frac{1}{2}}. \tag{3.3}$$

Thus, our model for the dynamic permeability/tortuosity is

$$\tilde{\alpha}(\omega) = \alpha_\infty + \frac{i\eta\phi}{\omega k_0\rho_f}\left\{1 - \frac{4i\alpha_\infty^2 k_0^2\rho_f\omega}{\eta\Lambda^2\phi^2}\right\}^{\frac{1}{2}}, \tag{3.4a}$$

$$\tilde{k}(\omega) = \frac{k_0}{\left\{1 - \frac{4i\alpha_\infty^2 k_0^2\rho_f\omega}{\eta\Lambda^2\phi^2}\right\}^{\frac{1}{2}} - \frac{i\alpha_\infty k_0\rho_f\omega}{\eta\phi}}. \tag{3.4b}$$

Equations (3.4a, b) are the central result of this paper. We wish to compare the accuracy of this model against other, known, results. First, we consider a hypothetical porous medium in which the pores are circular cylindrical tubes of radius c_0 canted at an angle θ to the imposed pressure drop; the response is given by (2.20b) from which it is simple to deduce the entity $F(\omega)$, defined by (3.1):

$$F_{\mathrm{CCT}}(\omega) = \frac{-2ixJ_1(4(ix)^{\frac{1}{2}})}{2(ix)^{\frac{1}{2}}J_0(4(ix)^{\frac{1}{2}}) - J_1(4(ix)^{\frac{1}{2}})}, \tag{3.5}$$

where $x = c_0^2\rho_f\omega/16\eta$. For this particular geometry, the relations (2.22) hold so that (3.3) becomes $F(\omega) = (1-ix)^{\frac{1}{2}}$. In figure 1 we compare the fractional difference, $2[F_{\mathrm{CCT}}(x) - F(x)]/[F_{\mathrm{CCT}}(x) + F(x)]$ as a function of x. By construction this difference is identically zero at high and low frequencies and we see that there is only a 10% difference at most in the middle-frequency range. Equation (3.5) or, equivalently, (2.20), is widely used, without particular justification, in the study of acoustics in porous media (Stoll 1974); we maintain that essentially any function which satisfies the general properties of §2 will do just as well as any other, in particular (3.4) or (2.20).

Next, we consider a simple cubic lattice of lattice constant l on which we randomly distribute tubes between the nodes thereof using some distribution function $P(r)$. As an aside, if all the tubes are the same, $P(r) = \delta(r - c_0)$, then the dynamic permeability/tortuosity is the same as for a collection of straight tubes, (2.20) with $\theta = 0$, except that only one third of them are conducting, i.e.

$$\tilde{\alpha}(\omega) = \frac{3}{\left[1 - \frac{2J_1(Kc_0)}{Kc_0 J_0(Kc_0)}\right]}. \tag{3.6}$$

We note that $\alpha_\infty = 3$ independent of the tube size and, in fact, we shall consider the value of α_∞ to be a measure of the disorder in the system. We have already demonstrated the validity of our model compared to (3.6), as was shown in figure 1.

For cases in which $P(r)$ is non-trivial, we have solved for the dynamic permeability by direct simulation on large ($10 \times 10 \times 10$) lattices and we have averaged over many (100) realizations as described elsewhere (Koplik 1981); at any frequency, and for any

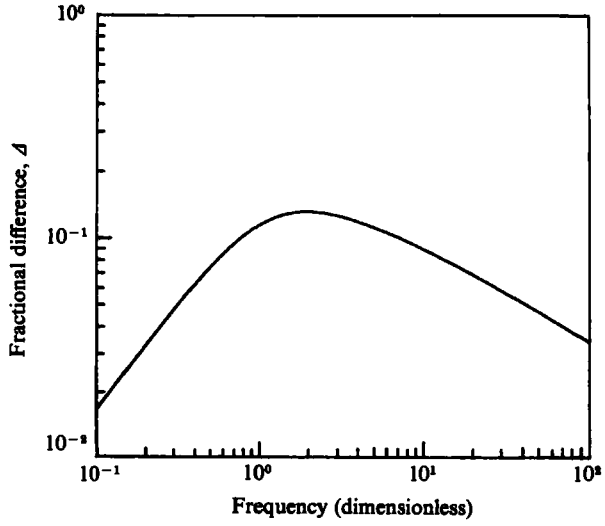

FIGURE 1. Comparison of the fractional difference, $|2[F_{CCT}-F]/[F_{CCT}+F]|$, as a function of dimensionless frequency, $x = (\rho\omega/\eta)[2\alpha_\infty k_0/(\Lambda\phi)]^2$. F_{CCT} is that appropriate to circular cylindrical tubes of radius R, equation (2.20a); F is the proposed model of the present article, equation (3.3).

individual tube, the fluid conductance is given by (2.19) in terms of the pressure difference between two connected nodes. The d.c. permeability k_0 is determined by a separate simulation for $\omega = 0$; $\dot{V} = [r^4/8\eta l]\Delta P$ for each tube. The porosity is simply $\phi = 3\int \pi r^2 l P(r)\,dr/l^3$. As indicated in §2, α_∞ and Λ are determined from a separate simulation of the electrical conductivity problem in which the current in a given bond is related to the voltage difference between the nodes by

$$I = g(V_i - V_j), \quad g(r) = \frac{\pi r^2}{l}. \tag{3.7a,b}$$

Because of (2.8), α_∞ is simply related to $\bar{g}$, the equivalent bond electrical conductivity of the random network, by

$$\alpha_\infty = 3\frac{\langle g\rangle}{\bar{g}}, \tag{3.8a}$$

where $\langle g\rangle$ is simply the arithmetic mean of the conductances

$$\langle g\rangle = \int g(r)\,P(r)\,dr. \tag{3.8b}$$

Equations (3.8a,b) follow directly from (2.8) because $F = l/\bar{g}$. A very 'tortuous' (i.e. disordered) network is one in which the effective conductivity is much smaller than the mean, $\alpha_\infty \gg 3$. Having solved for the voltages V_i at each node we can very simply evaluate Λ from (2.17):

$$\Lambda = \frac{\sum_{ij} (V_i - V_j)^2 r_{ij}^2}{\sum_{ij} (V_i - V_j)^2 r_{ij}}. \tag{3.9}$$

What sort of distribution $P(r)$ ought we to consider? Clearly we would like one for which α_∞ is appreciably larger than 3. In a previous simulation of the electrical conductivity using a rectangular distribution of conductances

$$Q(g) = \begin{cases} \frac{1}{4999} & 1 < g < 5000 \\ 0 & \text{otherwise,} \end{cases} \tag{3.10}$$

it was found that $\bar{g} = 2182$ for the simple cubic lattice (Koplik 1981); this gives a value for the tortuosity α_∞ of 3.44, which is not very different from that for an ordered lattice. In order to increase the disorder we wish to use a distribution which emphasizes the smaller conductors; to be specific, we consider the distribution

$$P(r) = \frac{1}{c_0} e^{-r/c_0}. \tag{3.11}$$

The porosity of this network is $\phi = 6\pi(c_0/l)^2$. We find the d.c. permeability to be $k_0 = (0.41 \pm 0.05)(c_0^2/l)^2$. (The error bars are statistical.) From the simulation of the electrical conductivity we find $\alpha_\infty = 7.94 \pm 0.47$; this value is considerably larger than those actually measured on a collection of fused glass-bead samples (Johnson *et al.* 1982; Wong, Koplik & Tomanic 1984) for which $10\% < \phi < 35\%$, giving us confidence that this simulation represents an appreciably disordered system. From the same electrical simulation we find $\Lambda = (0.93 \pm 0.10)c_0$. The relatively large error bars in Λ are systematic; the value of Λ depends on whether the conductors adjacent to the bus bars are included in (3.9) or not. This can be understood as follows. In principle, for an extremely large sample, (3.9) is independent of the thickness of the slab over which the summation is taken. Suppose the summation is limited to include only those conductors which are connected to the bus bars. For those conductors the fluctuations in the voltage drops, $V_i - V_j$, are smaller than for conductors in the bulk (because the end connected to the bus bar cannot fluctuate). If we completely neglect fluctuations in the voltage drop, then $\Lambda = 2c_0$ for the distribution (3.11). Therefore, inclusion of the end conductors tends to increase the value of Λ over that obtained without their inclusion; this effect is reflected in the error bars that we quoted for Λ, above. We have found that this effect does diminish as the sample length is increased.

Before we compare these numerical results against the model (3.4), we should like to make two observations about the values of the parameters themselves. (*a*) The value of Λ is considerably smaller than that deduced from the specific area; we find $2/\Lambda = 2.15/c_0$ whereas the surface-to-pore-volume ratio is $1/c_0$. Evidently the weighting procedure implied by (2.17) substantially favours the smaller tubes. (*b*) As regards the approximate validity of (2.22) with the values determined above, we find $8\alpha_\infty k_0/\phi\Lambda^2 = 1.6$ instead of 1.0. One can judge for oneself whether the glass is half full or half empty.

As a further check of (2.22) we have considered other distributions which also tend to emphasize the smaller conductors. For example, simulations based on the divergent distribution $\{P(r) = \frac{1}{2}(c_0 r)^{-\frac{1}{2}}: 0 < r < c_0\}$, for which $\phi = (3\pi/5)(c_0/l)^2$, give $k_0 = 0.0085c_0^4/l^2$, $\alpha_\infty = 6.2$, and $\Lambda = 0.33c_0$ from which it follows that $8\alpha_\infty k_0/\phi\Lambda^2 = 2.0$ for this distribution. For this distribution, too, we find the value of $2/\Lambda\,(= 6.0/c_0)$ to be much larger than the surface-to-pore-volume ratio $(= 3.33/c_0)$. We conclude that it will be quite difficult to find any probability distribution $P(r)$ for which (2.22) is violated by more than an order of magnitude. In fact, it is instructive to consider an arbitrary distribution of tubes having different radii (same length) connected in series and in parallel. We find that for tubes connected in parallel

$$k_0 = \frac{\phi\langle R^4\rangle}{8\langle R^2\rangle}, \quad \alpha_\infty = 1.0, \quad \Lambda = \frac{\langle R^2\rangle}{\langle R\rangle}.$$

Thus

$$M = \frac{\langle R^4\rangle\langle R\rangle^2}{\langle R^2\rangle^3},$$

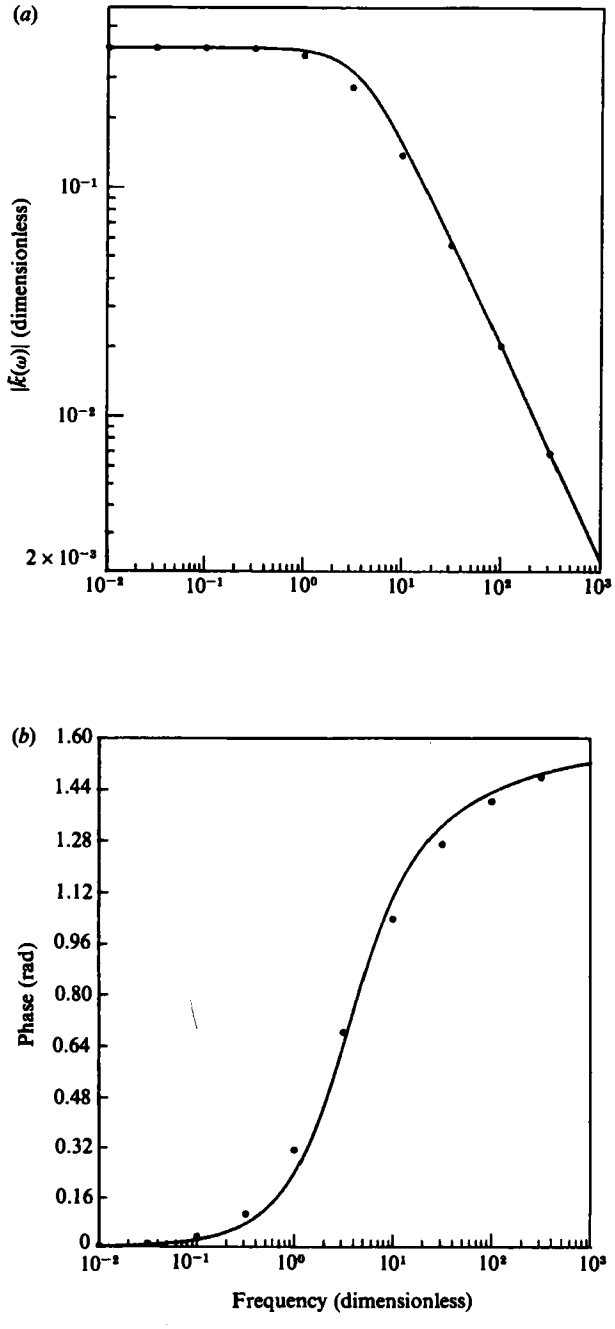

FIGURE 2. (*a*) Absolute value, in units of c_0^4/l^2, and (*b*) phase of the dynamic permeability of a random network of tubes distributed on the bonds of a simple cubic lattice using the exponential probability distribution of tube radii. The dimensionless frequency is $\omega\rho c_0^2/\eta$. The points are the results of direct simulations. The solid curves are the predictions of the model dynamic permeability, equation (3.3). The input parameters for the model, k_0, α_∞, and Λ, were determined by means of separate simulations, as explained in the text. $P(r) = (1/c_0)/e^{-r/c_0}$; $\phi = 6\pi(c_0/l)^2$; $k_0 = 0.41c_0^4/l^2$; $\alpha_\infty = 7.9$; $\Lambda = 0.89c_0$.

where $M \equiv 8\alpha_\infty k_0/\phi\Lambda^2$. Similarly, for tubes connected in series

$$k_0 = \frac{\phi}{8\langle R^2\rangle\langle R^{-4}\rangle}, \quad \alpha_\infty = \langle R^{-2}\rangle\langle R^2\rangle, \quad \Lambda = \frac{\langle R^{-2}\rangle}{\langle R^{-3}\rangle},$$

which implies

$$M = \frac{\langle R^{-3}\rangle^2}{\langle R^{-4}\rangle\langle R^{-2}\rangle}.$$

Although the two expressions for M are different, it is clear that in the parallel case all the moments are dominated by the largest tubes, with the result that $M \to 1$ and in the series case all the moments are dominated by the smallest tubes, with the result that, again, $M \to 1$. We have not been able to find a striking counterexample to $M \approx 1$, which is surprising since at some point the analogy between potential flow and Poiseuille flow must break down.

In figure 2(a, b) we plot the magnitude and phase, respectively, of the dynamic permeability deduced from the numerical simulations using the exponential distribution. We also compare these results with the predictions of the simple model, (3.4). Once again, we see that the model dynamic permeability agrees very well with that calculated directly; there are no adjustable parameters in the model, all of them having been calculated independently.

We hasten to point out that we have invented a model $\tilde{k}(\omega)$ which correctly matches the frequency dependence of the first two leading terms of the exact result for high frequencies (2.16), but only one term for low frequencies (2.6). Thus if we expand about $\omega \sim 0$ we have

$$\tilde{k}(\omega) = k_0 + i\omega\beta + O(\omega^2). \tag{3.12}$$

The point is that our model (3.4), may very well yield values of β that differ substantially from the exact values. We have been unable to find any rigorous theoretical statements that can be made about this coefficient. However, β appears not to be directly measurable in any experimental situation, except as a correction to the d.c. behaviour. To some extent this has happened in the experiments considered by Attenborough (1983); it would be interesting to compare the low-frequency behaviour of these systems with the predictions of our model, (3.4), using values of Λ deduced from superfluid ^{4}He experiments (§5, below).

Finally, we consider the case in which $P(r)$ corresponds to classical bond percolation theory (Kirkpatrick 1973): $P(r) = p\delta(r-c_0) + (1-p)\,\delta(r)$. A fraction p of the bonds are occupied by tubes of the same radius c_0, and the rest are empty. It is clear that the dynamic permeability at any frequency is simply related to (2.20b) by a geometrical factor independent of frequency:

$$\tilde{k}(\omega) = G(p)\,\frac{\phi\eta}{3i\omega\rho_f}\left[\frac{2J_1(Kc_0)}{Kc_0 J_0(Kc_0)} - 1\right], \tag{3.13}$$

where $G(p)$ is dependent only on p (for a given lattice type) and has the property that $G(1) = 1$ and G vanishes whenever p is less than the percolation threshold. Inasmuch as we have already seen that the simple model (3.4), agrees well with (2.20) for a single tube, we automatically have good agreement for the percolation problem, too, as long as α_∞ and k_0 are scaled with $G(p)$ so that they take on their correct values. We note that any p, $\Lambda \equiv c_0$, as is obvious from (3.9). Therefore, the relationship $8\alpha_\infty k_0/\phi\Lambda^2 \equiv 1$ holds for arbitrary p.

The conclusion of this section is that we have found a simple analytic expression for the frequency dependence of the permeability/tortuosity in terms of the well-defined (and experimentally measurable) high- and low-frequency parameters.

The model is the rough equivalent of the Debye model for relaxation phenomena in dielectric properties (Frohlich 1949). Compared with direct simulations on large networks, the model works well for a narrow distribution of tube radii, $P(r) = \delta(r-c_0)$, a wide distribution of tube radii, $P(r) = c_0^{-1} \exp(-r/c_0)$, and the bimodal distribution corresponding to percolation theory, $P(r) = p\delta(r-c) + (1-p)\,\delta(r)$. We conclude that unless the distribution is pathological (having a divergence at $r = 0$) the model will continue to given an accurate description of the frequency dependence of the permeability. It is likely that other simple forms will work as well as the one considered here.

We also conclude, based on direct calculations of the parameters themselves, that the Λ parameter is closely related to the d.c. permeability k_0, through (2.22), at least for random lattice networks; the relationship (2.22) may be violated by a factor of 2 but not, apparently, a factor of 10. This also seems to hold true for the available experimental data, which we discuss in §5.

4. Relation to acoustics in deformable porous media

In this section we relax the assumption that the solid is not deformable and we consider the relevance of our results to the acoustic properties of porous media generally. It has become clear that the Biot theory (Biot 1956*a*, *b*, 1962*a*, *b*; Biot & Willis 1957) is the appropriate basic theory for such systems, although, of course, there are porous media that exhibit effects which are dominated by mechanisms outside the Biot theory; the equivalent statement for non-porous media is that standard elasticity theory, based on Hookian springs between atoms, is the appropriate basic theory of acoustics therein, although there are many mechanisms for attenuation and dispersion in real systems which lie outside standard elasticity proper. The basic idea of the Biot theory is that the average displacement of the fluid, $\boldsymbol{U}(\boldsymbol{r}, t)$, and of the solid, $\boldsymbol{u}(\boldsymbol{r}, t)$ are followed separately and on an equal footing, although the two motions are coupled. As a consequence, two distinct longitudinal modes at all frequencies are predicted, a 'fast' wave and a 'slow' wave; although the former is propagatory at all frequencies, the latter is diffusive at low frequencies and propagatory at high. The theory has been successfully applied to such disparate systems as fourth sound in a superfluid/superleak system (Johnson 1980), pressure diffusion through porous media (Chandler & Johnson 1981), slow waves and the consolidation transition (Johnson & Plona 1982), elastodynamics of gels (Johnson 1982), as well as the acoustic properties of 'ordinary' porous media saturated with 'ordinary' fluids (Johnson *et al.* 1982). Especially for these latter systems, the Biot theory has tremendous predictive power in the sense that a given sample can be characterized by direct and independent measurement of most of the input parameters which are then used to predict the speeds and attenuations of the modes, regardless of what pore fluid is used. Aside from the densities and moduli of the fluid and solid constituents, the parameters are the porosity ϕ, and the moduli of the skeleton frame K_b and N, which can be deduced from the measured speeds of the dry material. The strictly low-frequency properties are dependent on the value of the permeability k_0, and the strictly high-frequency properties are dependent on the value of the tortuosity α_∞. The distinction between high and low frequencies is whether the drag that the solid exerts on the fluid is dominated by inertial or by viscous effects, respectively. The predicted velocities have been verified experimentally in both limits. These and other properties of the theory are reviewed elsewhere (Johnson 1984; Stoll 1974).

The missing ingredient is a simple description of the viscous/inertial drag effects which can be expected to be valid over the entire frequency range in terms of a few independently measurable parameters characteristic of a given sample. In the Biot theory, these effects are described in terms of the relative motion between fluid and solid; the equation of motion for the fluid constituent can be written (Johnson & Plona 1982; Johnson 1984)

$$\phi\rho_{\mathrm{f}}\frac{\partial^2\boldsymbol{U}}{\partial t^2}=\tilde{\rho}_{12}(\omega)\left[\frac{\partial^2\boldsymbol{U}}{\partial t^2}-\frac{\partial^2\boldsymbol{u}}{\partial t^2}\right]+(\text{spatial derivative terms}), \tag{4.1a}$$

where

$$\tilde{\rho}_{12}(\omega)=-[\tilde{\alpha}(\omega)-1]\phi\rho_{\mathrm{f}}. \tag{4.1b}$$

The quantity $\tilde{\alpha}(\omega)$ appearing in (4.1 *b*) is independent of the elastic properties of the two constituents and is, in fact, identical with that defined in (2.1 *a*). This can be seen by considering the Biot equations in the limit that the skeletal frame moduli, K_b and N, are much larger than the bulk modulus of the fluid, so that the solid does not move ($\boldsymbol{u}\equiv 0$); in this limit, (4.1 *a*, *b*) reduce identically to (2.1 *a*).

The implications are that the general properties of $\tilde{\alpha}(\omega)$ deduced in §2 automatically apply to the acoustics of porous media generally, via the Biot theory. Moreover, we have derived a simple theory, (3.4 *a*), which gives a good description of $\tilde{\alpha}(\omega)$ in a substantially disordered system over the entire frequency range, as was shown in figure 2(*a*, *b*). One now has the confidence, once values for α_∞, Λ, k_0, and ϕ are measured, that there is a reliable means of calculating the acoustic properties over the full frequency spectrum.

The conventional approach has been to treat the pore space as if it were equivalent to circular tubes of some effective radius (Biot 1956; Stoll 1974), i.e. by means of (2.20) or equivalently (3.5). The effective tube radius is derived from the measured permeability by means of (2.22). The argument of the Bessel functions is then modified by multiplicative 'structure factors' n^2/s or $\delta^2/8\xi$ which, in the language of the present article, allows for a value of Λ which does not satisfy (2.22). Although such a procedure may seem to be an *ad hoc* one, in fact the set of free parameters is still four in number and, moreover, the specific functional form (2.20) is numerically quite similar to, say, the present model, (3.4 *a*, *b*), for real-valued frequencies. The simple reason is that essentially any function satisfying the conditions of §2 will agree with any other function for real ω. Indeed, it was noted long ago that $F(\omega)$ for the case in which the pores are modelled as flat slabs, also agree quite well with (2.20) for real ω (Biot 1956). Obviously, all these formulae are very different for ω on the negative imaginary axis, where they have singularities.

5. Superfluid acoustics as a probe of porous media

Below a temperature $T_\lambda = 2.17$ K, liquid ^{4}He undergoes a transition to a new phase, He II, which behaves as a miscible mixture of a normal fluid having a viscosity η and a density $\rho_{\mathrm{N}}(T)$, and a superfluid fraction having exactly zero viscosity and a density $\rho_{\mathrm{S}}(T)$; obviously $\rho_{\mathrm{N}}(T)+\rho_{\mathrm{S}}(T)=\rho$. The properties of He II, and especially the two-fluid equations of motion, are described simply by Tilley & Tilley (1974). The acoustic properties are reviewed by Rudnick (1976) and dissipative effects are discussed quite clearly by Putterman (1974). For this section only, we presume familiarity with the contents of these texts. The extraordinary success of the macroscopic two-fluid equations of motion in describing the bulk properties of He II was established in large measure by means of experiments using ^{4}He in porous media

and other confined geometries. It is the purpose of this section to turn this situation around and establish the use of superfluid acoustics as a powerful probe of porous media, specifically as a means of measuring $\tilde{k}(\omega)$.

As in §2 we assume that the ^{4}He is describable by its macroscopic equations of motion, negligibly affected by proximity to the walls of the porous medium. We also continue to neglect the thermal expansion coefficient of the ^{4}He. The linearized microscopic equations of motion are (Tilley & Tilley 1974; Putterman 1974):

$$\rho_{\mathrm{N}} \frac{\partial \boldsymbol{u}_{\mathrm{N}}}{\partial t} = -\frac{\rho_{\mathrm{N}}}{\rho} \nabla P - \rho_{\mathrm{S}} s \nabla T - \eta \nabla \times \nabla \times \boldsymbol{u}_{\mathrm{N}}, \tag{5.1a}$$

$$\rho_{\mathrm{S}} \frac{\partial \boldsymbol{u}_{\mathrm{S}}}{\partial t} = -\frac{\rho_{\mathrm{S}}}{\rho} \nabla P + \rho_{\mathrm{S}} s \nabla T, \tag{5.1b}$$

$$\nabla \cdot (\rho_{\mathrm{S}} \boldsymbol{u}_{\mathrm{S}} + \rho_{\mathrm{N}} \boldsymbol{u}_{\mathrm{N}}) + \frac{\partial (\rho_{\mathrm{N}} + \rho_{\mathrm{S}})}{\partial t} = 0, \tag{5.1c}$$

$$\nabla \cdot (\rho s \boldsymbol{u}_{\mathrm{N}}) + \frac{\partial (\rho s)}{\partial t} = 0, \tag{5.1d}$$

$$P = P_0 + \frac{\partial P}{\partial \rho} (\rho - \rho_0), \quad T = T_0 + \frac{\partial T}{\partial s} (s - s_0), \tag{5.1e,f}$$

where $\boldsymbol{u}_{\mathrm{N}}(\boldsymbol{r}, t)$ and $\boldsymbol{u}_{\mathrm{S}}(\boldsymbol{r}, t)$ are the velocity fields of the normal and superfluid fractions respectively, T is the temperature, P is the pressure, and s is the entropy per unit mass. In (5.1) we have included the dissipative effects of the normal-fluid viscosity, but have neglected the three 'second' viscosities as well as the thermal conductivity (see below). In the absence of a porous medium, there are two normal modes in He II: first sound, a pressure–density wave whose speed is $c_1^2 = \partial P / \partial \rho$ (approximately 240 m/s), and second sound, a temperature–entropy variation whose speed is $c_2^2 = (\rho_{\mathrm{S}} s_0^2 / \rho_{\mathrm{N}}) \partial T / \partial s$ (approximately 20 m/s). The attenuation of these modes in the bulk is governed by the neglected dissipative terms, as well as by η. In a porous medium whose pore sizes are much smaller than the wavelengths of first or second sound, these attenuation mechanisms are negligible compared to that caused by viscous shearing of the normal fluid inside each pore; for our purposes, we are justified in neglecting them.

At the internal walls of the porous medium, the boundary conditions are that the tangential component of the normal fluid must vanish, $\boldsymbol{u}_{\mathrm{N}} \times \hat{\boldsymbol{n}} = 0$, there is no momentum transfer into the solid, $(\rho_{\mathrm{S}} \boldsymbol{u}_{\mathrm{S}} + \rho_{\mathrm{N}} \boldsymbol{u}_{\mathrm{N}}) \cdot \hat{\boldsymbol{n}} = 0$, and there is no entropy flux into the solid, $\rho s_0 \boldsymbol{u}_{\mathrm{N}} \cdot \hat{\boldsymbol{n}} = 0$. This last is not true for a solid with a finite thermal conductivity, but it introduces a negligible error, as we show in Appendix B. On the scale of the pore sizes, the equation of motion for the superfluid fraction is

$$\rho_{\mathrm{S}} \frac{\partial \boldsymbol{u}_{\mathrm{S}}}{\partial t} = -\nabla \mu \tag{5.2a}$$

(where $\nabla \mu = (\rho_{\mathrm{S}} / \rho) \nabla P - \rho_{\mathrm{S}} s_0 \nabla T$) subject to the boundary condition

$$\boldsymbol{u}_{\mathrm{S}} \cdot \hat{\boldsymbol{n}} = 0 \tag{5.2b}$$

at the walls of the pores. Mathematically, this is identical with the equations for an ideal fluid occupying the pore space; therefore, the macroscopic flow rate of the superfluid fraction is given by

$$\alpha_\infty \rho_{\mathrm{S}} \frac{\partial \boldsymbol{v}_{\mathrm{S}}}{\partial t} = -\nabla \mu, \tag{5.3}$$

in which $\boldsymbol{v}_S$ is related to $\boldsymbol{u}_S$ in the same way as $\boldsymbol{v}$ is related to $\boldsymbol{u}$ in §2. Note that α_∞ is identical with that in (2.7). Similarly, the microscopic equation of motion for the normal-fluid fraction is

$$\rho_N \frac{\partial \boldsymbol{u}_N}{\partial t} = -\nabla\chi + \eta \nabla \times \nabla \times \boldsymbol{u}_N \tag{5.4a}$$

(where $\nabla\chi = (\rho_N/\rho)\nabla P + \rho_S s_0 \nabla T$), subject to the boundary condition

$$\boldsymbol{u}_N = 0 \tag{5.4b}$$

on the pore walls. This obviously maps onto the equations for a Newtonian fluid and so the macroscopic response of the normal component is

$$\tilde{\alpha}(\omega)\rho_N \frac{\partial \boldsymbol{v}_N}{\partial t} = -\nabla\chi. \tag{5.5}$$

The dynamic tortuosity entering (5.5) is the same as that defined in (2.1a) for a hypothetical Newtonian fluid of viscosity η and density $\rho_N(T)$.

It is now straightforward to solve for the normal modes of He II in a porous medium, using (5.3) and (5.5):

$$q_\pm^2 = \frac{\omega^2\{\Delta \pm (\Delta^2 - 4c_1^2 c_2^2 \alpha_\infty \tilde{\alpha}(\omega))^{\frac{1}{2}}\}}{2c_1^2 c_2^2}, \tag{5.6}$$

where

$$\Delta = \frac{\rho_S}{\rho}(\tilde{\alpha}(\omega)c_1^2 + \alpha_\infty c_2^2) + \frac{\rho_N}{\rho}(\alpha_\infty c_1^2 + \tilde{\alpha}(\omega)c_2^2).$$

Following Baker (1985, 1986), we observe that $(\rho_N/\rho_S)(c_2^2/c_1^2) < 0.01$ for all p and T. Therefore, to better the 1 % accuracy the normal modes simplify to

$$q_-^2 = \frac{\omega^2}{c_1^2}\left[\frac{\tilde{\alpha}(\omega)\alpha_\infty}{\alpha_\infty + (\alpha(\omega) - \alpha_\infty)\dfrac{\rho_S}{\rho}}\right], \tag{5.7}$$

$$q_+^2 = \frac{\omega^2}{c_2^2}\left[\alpha_\infty + (\tilde{\alpha}(\omega) - \alpha_\infty)\frac{\rho_S}{\rho}\right]. \tag{5.8}$$

It is clear that measurements of the speed and attenuation of these modes enable one to directly deduce $\tilde{\alpha}(\omega)$ although the existing data are either for the strictly high-frequency or strictly low-frequency limits. Let us consider these two limits implied by (5.7) and (5.8).

High frequencies. At sufficiently high frequencies (2.16) applies and so the dispersion in the phase velocity and the attenuation implied by (5.7) are

$$\lim_{\omega\to\infty} V_- = \frac{c_1}{(\alpha_\infty)^{\frac{1}{2}}}\left[1 - \frac{\rho_N}{\rho}\frac{\delta(\omega, T)}{2\Lambda}\right], \tag{5.9a}$$

$$\lim_{\omega\to\infty} \frac{1}{Q_-} = \frac{\rho_N}{\rho}\frac{\delta(\omega, t)}{\Lambda}, \tag{5.9b}$$

where $\delta = (2\eta/\rho_N\omega)^{\frac{1}{2}}$. Similarly (5.8) gives

$$\lim_{\omega\to\infty} V_+ = \frac{c_2}{(\alpha_\infty)^{\frac{1}{2}}}\left[1 - \frac{\rho_S}{\rho}\frac{\delta(\omega, T)}{2\Lambda}\right], \tag{5.10a}$$

$$\lim_{\omega\to\infty} \frac{1}{Q_+} = \frac{\rho_S}{\rho}\frac{\delta(\omega, T)}{\Lambda}. \tag{5.10b}$$

In this limit the modes are essentially first and second sound but with speeds reduced by the factor $(\alpha_\infty)^{\frac{1}{2}}$ because of the tortuous, winding pore space. Obviously, (5.9*b*) and (5.10*b*) are the analogues of (2.18) for He II. The temperature and frequency dependences in (5.9) and (5.10) have been reported by Singer *et al.* (1985) for five samples of fused glass beads. Baker (1985) has also made similar measurements on a set of three samples of sintered bronze spheres. In particular, values of the parameter Λ (r in the notation of Singer *et al.* and $(8/\delta)\,(k\alpha/P)^{\frac{1}{2}}$ in Baker's notation) have been measured.

Baker (1986) has independently measured ϕ, α_∞, k_0 on his samples. He has experimentally deduced values for Λ from measurements of Q_-. Does (2.22) hold for those samples? In our notation the quantity $8\alpha_\infty k_0/(\phi\Lambda^2)$ of (2.22) is $\delta^2/8$ in his. From table 1 of Baker (1986) $\delta^2/8$ varies from 1.4 to 2.5, which is comparable with the values that we found from the network simulations in §3 (i.e. 1.6 and 2.0). This, then, is direct experimental evidence that the Λ parameter is closely related to d.c. permeability k_0, in real porous media.

Low frequencies. In this limit, the mode corresponding to first sound at high frequencies, (5.7), has a speed and attenuation given by

$$\lim_{\omega\to 0} V_- = \left(\frac{\rho_S}{\rho}\right)^{\frac{1}{2}} \frac{c_1}{(\alpha_\infty)^{\frac{1}{2}}}, \tag{5.11a}$$

$$\lim_{\omega\to 0} \frac{1}{Q_-} = \frac{\alpha_\infty k_0 \rho_N^2 \omega}{\phi\eta\rho_S}. \tag{5.11b}$$

This is fourth sound, a mode that exists whenever the normal component is clamped ($v_N \equiv 0$) by virtue if its viscosity. It was first observed by Shapiro & Rudnick (1965). This crossover from first sound at high frequencies to fourth sound at low was predicted by Shapiro & Rudnick who did not, however, present a complete description of the effects of the porous medium, i.e. their treatment is equivalent to the assumption that $\tilde{k}(\omega) = k_0$ is constant for all frequencies. Kriss (1969) and, more recently, Tam & Ahlers (1985) have experimentally verified the temperature and frequency dependence of (5.11*b*) though they did not report independent measurements of k_0 (which is expressed as $k_0/\phi = a^2/8$, in their notation).

In this low-frequency limit, the second sound mode becomes diffusive in character, $q_+^2 = \mathrm{i}\omega/D$, with a diffusivity given by

$$D = \frac{\rho_N k_0}{\eta\phi}\left\{\frac{\rho_S/\rho}{c_2^2} + \frac{\rho_N/\rho}{c_1^2}\right\}^{-1}. \tag{5.12}$$

Like second sound this is essentially a temperature/entropy wave with a small admixture of pressure/density. Theoretical descriptions of this mode have been presented by others using simplifying assumptions about the geometry of the porous medium (Pollack & Pellam 1965; Shapiro & Rudnick 1965; Weichert & Meinhold-Heerlein 1970). This mode was unambiguously observed by Weichert & Passing (1982) in plane-parallel capillaries of width $2d$ for which $k_0/\phi = d^2/3$. In a porous medium it ought to be straightforward to observe this mode using techniques similar to those of Chandler (1981) but with second-sound transducers.

We stress that the parameters α_∞ and k_0/ϕ, which determine the speed and attenuation of fourth sound, as well as the diffusivity of the thermal wave, are easily measurable using standard techniques of electrical conductivity and fluid-flow resistance (Baker 1985, 1986). In addition, α_∞ determines the high-frequency speed of first sound (Johnson *et al.* 1982) as well as that of second sound (Singer *et al.* 1984).

To summarize this section, we have seen that superfluid ^{4}He enables one in principle to measure $\tilde{k}(\omega)$ in a direct manner on a given sample; in practice, measurements have been limited to either the strictly high- or strictly low-frequency limits. There are four properties of He II which make it a powerful probe of acoustics in porous media:

(*a*) It is several orders of magnitude more compressible than most solids, making the rigid-frame approximation accurate to 1 part in 10^4, typically (Johnson 1980).

(*b*) The normal-fluid fraction ρ_N/ρ can be made to be arbitrarily small simply by going to a low enough temperature; below 1.2 K, the normal-fluid fraction is less than 1 %. This enables a direct acoustical measurement of α_∞ from (5.9*a*) or (5.11*a*), which are the same.

(*c*) Although the viscosity of the normal component η is not very temperature dependent, the effects of viscosity can be varied considerably by changing the temperature; because the normal-fluid fraction decreases from unity to zero, the viscous skin depth $(2\eta/\rho_N\omega)^{\frac{1}{2}}$ diverges at low temperature.

(*d*) Since there are two distinct sound modes in He II, (5.7) and (5.8), one can extend the spectral range simply by switching from a first-sound transducer to a second-sound transducer; in a typical resonant-cavity experiment the wavelength is fixed by the cavity dimensions, so that a change from first to second sound changes the resonant frequency by a factor of ten (i.e. c_1/c_2).

6. Fractal pore surfaces

A recent article (Katz & Thompson 1985) provided compelling evidence from direct scanning electron microscope images that the pore–grain interface in many sedimentary rocks is an object having a fractional dimensionality greater than two over a range of lengthscales from 100 Å to 100 μm. Earlier work using gas adsorption data indicated a similar result but was limited to much smaller lengthscales (Avnir, Farin & Pfeiffer 1984). The basic idea of a fractal surface is that if one measures the area using a 'yardstick' of length δ, the area will diverge as δ shrinks to zero according to a power law, $A \propto \delta^{2-d}$, where d (> 2) is the fractal dimension (Mandelbrot 1982). In the case at hand, the yardstick is the viscous skin depth $\delta = (2\eta/\rho_f\omega)^{\frac{1}{2}}$. As a point of information, the viscous skin depth in water at 1 MHz is $\delta = 0.6$ μm; the viscous skin depth of the normal component in He II at, say, $T = 1.8$ K and $f = 10^4$ kHz, is $\delta = 0.9$ μm. These values are in an experimentally accessible range for probing the pore structure of the sedimentary rocks considered by Katz & Thompson. In this section we consider the implications of a fractal pore–grain interface on the dynamic tortuosity. We assume, however, that the pore volume itself is three-dimensional.

Consider the high-frequency limit (2.16), which was derived under the assumption that the bounding surface of the fluid appears flat locally if the viscous skin depth is small enough. If, however, the surface is a fractal object, then as δ decreases with increasing frequency, the fluid 'sees' an increasing surface area, as indicated schematically in figure 3. The parameter Λ presumably decreases with decreasing δ: $2/\Lambda \sim \delta^{2-d_\Lambda}$. Under these assumptions, (2.16) becomes

$$\lim_{\omega\to\infty} \tilde{\alpha}(\omega) = \alpha_\infty \left(1 + \left[\frac{2}{\Lambda_f}\left(\frac{i\eta}{\rho_f\omega}\right)^{\frac{1}{2}}\right]^{3-d_\Lambda}\right), \tag{6.1}$$

where Λ_f has the dimensions of length and α_∞ is related, as before, to the electrical conductivity. We note that d_Λ is not really the fractal dimension of the pore surface; (6.1) describes a dynamic process and it is unlikely that the exponent should be simply

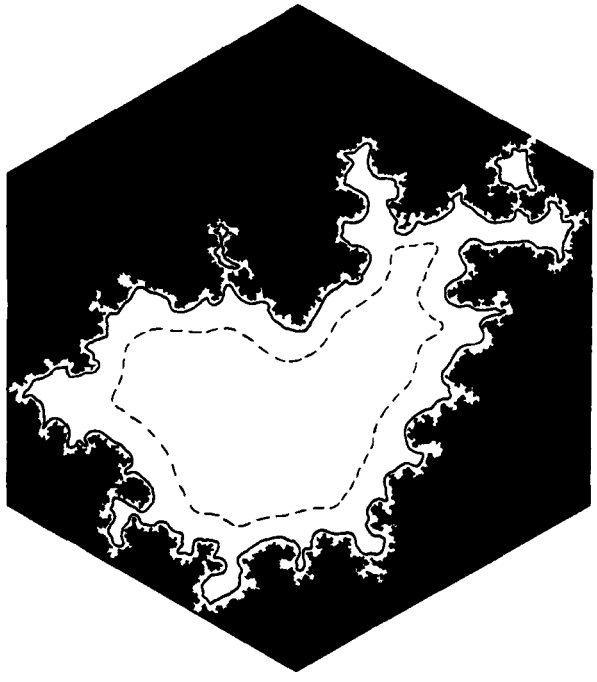

FIGURE 3. Schematic of a hypothetical fractal surface separating the fluid region (white) from the solid (black). With increasing frequency the viscous skin depth decreases and the boundary between potential flow (in the interior of the boundary) and Poiseuille flow effectively 'sees' an increasingly larger surface area. The solid line is for a considerably higher frequency than the dashed. Copyright by B. B. Mandelbrot, plate 231 in his *Fractal Geometry of Nature* (W. H. Freeman, New York, 1982), reprinted with permission.

related to static, purely geometrical properties, cf. the definition of Λ (2.17). Since $\boldsymbol{u}_{\mathrm{p}}$ becomes small within the peak height of the fractal surface, we anticipate $2 < d_{\Lambda} < d$.

It is straightforward to work out the implications for the normal modes using (6.1). The high-frequency limit for the specific attenuation is, similarly to (2.18),

$$\lim_{\omega\to\infty}\frac{1}{Q} = 2^{\frac{3-d_{\Lambda}}{2}}\sin\tfrac{1}{4}\pi\,(3-d_{\Lambda})\left[\frac{1}{\Lambda_{\mathrm{f}}}\left(\frac{2\eta}{\rho_{\mathrm{f}}\omega}\right)^{\frac{1}{2}}\right]^{3-d_{\Lambda}}. \tag{6.2}$$

From the results of the last section, it is clear that these effects are most easily seen using He II. In this high-frequency limit, then, the specific attenuation of first and second sounds are obtained by substitution of (6.1) into (5.7) and (5.8):

$$\lim_{\omega\to\infty}\frac{1}{Q_1} \propto \frac{\rho_{\mathrm{N}}(T)}{\rho}\left[\frac{2\eta}{\rho_{\mathrm{N}}(T)\,\omega}\right]^{\frac{3-d_{\Lambda}}{2}}, \tag{6.3a}$$

$$\lim_{\omega\to\infty}\frac{1}{Q_2} \propto \frac{\rho_{\mathrm{S}}(T)}{\rho}\left[\frac{2\eta}{\rho_{\mathrm{N}}(T)\,\omega}\right]^{\frac{3-d_{\Lambda}}{2}}. \tag{6.3b}$$

In principle, the dynamic dimensionality of the pore–grain interface d_{Λ} can be deduced from either the temperature or frequency dependence of the attenuation of first and/or second sound in a porous medium.

What, then, might one expect for the full frequency dependence of the dynamic tortuosity? We note that, since we assumed that the pore volume is three-dimen-

sional, the d.c. permeability is well defined and measurable; (2.6a, b) still hold. Repeating the derivation of §3, but with (6.1) instead of (2.16), we conjecture that the dynamic tortuosity of such a system may be described by

$$\tilde{\alpha}(\omega) = \alpha_\infty + \frac{\mathrm{i}\eta\phi}{\omega k_0 \rho_\mathrm{f}}\left[1 - \beta\frac{\mathrm{i}\rho_\mathrm{f}\omega}{\eta}\right]^{(a_\Lambda - 1/2)}, \tag{6.4}$$

where β is related to Λ_f in order that (6.4) satisfies (6.1).

We are grateful for several useful discussions with H. Kojima, E. J. Hinch, and S. Baker.

Appendix A. Singularities of response functions

We consider the response of a system defined in §2. Specifically, we wish to show that $\tilde{\alpha}(\omega)$ and $\tilde{k}(\omega)$ are analytic functions of ω everywhere in the complex plane except for values of ω on the negative imaginary axis. We assume that the sample occupies the space $0 < x < L$ and its pore space is saturated with an incompressible Newtonian fluid; the linearized equations of motion are (Landau & Lifshitz 1959, p. 49)

$$\rho_\mathrm{f}\frac{\partial u_i}{\partial t} = T_{ij,\,j}, \tag{A 1a}$$

where

$$T_{ij} = \eta Q_{ij} - \delta_{ij} P, \quad Q_{ij} = u_{i,\,j} + u_{j,\,i} \tag{A 1b,c}$$

(a comma denotes differentiation and summation over repeated indices is assumed). The microscopic velocity field $\boldsymbol{u}(\boldsymbol{r}, t)$ is related to the macroscopic $\boldsymbol{v}$ by considering the flow through an area A over which $\boldsymbol{v}$ is slowly varying: $\phi \boldsymbol{v}\cdot\hat{\boldsymbol{n}}A = \int \boldsymbol{u}\cdot\hat{\boldsymbol{n}}\,\mathrm{d}A$. We shall need the following (simple to verify) identity:

$$u_j^* T_{ij,\,i} = (u_j^* T_{ij})_{,\,i} - \tfrac{1}{2}\eta Q_{ij}^* Q_{ij}. \tag{A 2}$$

Next, we prove a theorem about the unforced oscillations in the system: Consider solutions to (A 1) in which all quantities have the same sinusoidal time dependence, e.g. $\boldsymbol{u}(\boldsymbol{r}, t) = \boldsymbol{u}(\boldsymbol{r})\,\mathrm{e}^{-\mathrm{i}\omega t}$ subject to the boundary condition

$$\int n_i u_j^* T_{ij}\,\mathrm{d}S = 0, \tag{A 3}$$

where the integration is over the multiply-connected boundary surface of the fluid including the planes $x = 0$ and $x = L$; $\hat{\boldsymbol{n}}$ is a unit vector normal to that surface at each point. (This is automatically guaranteed for the internal boundaries at the fluid–solid interface because $\boldsymbol{u} \equiv 0$. Equation (A 3) is a statement about the boundaries of the fluid at $x = 0$ and $x = L$.) This boundary condition guarantees that no power is entering the system.

THEOREM. *All solutions to the linearized Navier–Stokes equations subject to the boundary condition* (*A* 3) *have the property that* ω *is on the negative imaginary axis.*

Proof. From the equation of motion (A 1a, b) we have

$$-\mathrm{i}\omega\rho_\mathrm{f}\int u_i^* u_i\,\mathrm{d}V = \int u_i^* T_{ij,\,j}\,\mathrm{d}V, \tag{A 4}$$

where the integration is over the volume actually occupied by fluid in the region $0 < x < L$. Because of the identity (A 2), (A 4) becomes

$$-\mathrm{i}\omega\rho_{\mathrm{f}}\int u^* u\,\mathrm{d}V = \int \{u_i^* T_{ij}\}_{,j}\,\mathrm{d}V - \tfrac{1}{2}\eta\int |Q|^2\,\mathrm{d}V$$

$$= \int n_i u_j^* T_{ij}\,\mathrm{d}S - \tfrac{1}{2}\eta\int |Q|^2\,\mathrm{d}V. \tag{A 5}$$

Therefore, because of (A 3), the frequency is

$$\omega = \frac{-\mathrm{i}\eta}{2\rho_{\mathrm{f}}}\frac{\int |Q|^2\,\mathrm{d}V}{\int |u|^2\,\mathrm{d}V} \tag{A 6}$$

and the theorem is proved.

Consider, now, (2.1*a*) where $\tilde{\alpha}(\omega)$ is defined. A singularity in $\tilde{\alpha}(\omega)$ means that there exists a non-trivial solution to the Navier–Stokes equation on a microscopic scale having the property that $v = 0$. This occurs if the front and back surfaces of the sample (at $x = 0$ and $x = L$) are sealed off so that no fluid can cross these boundaries. This guarantees that $u(x = 0) = u(x = L) = 0$ thus fulfilling the boundary condition (A 3). Because of the theorem, such a situation has a non-trivial solution for ω only on the negative imaginary axis. Therefore, poles in $\tilde{\alpha}(\omega)$ occur only on the negative imaginary axis.

Similarly (2.1*b*) shows that a pole of $\tilde{k}(\omega)$ implies the existence of a non-trivial microscopic solution having the property that the macroscopic pressure gradient vanishes. On a microscopic scale, we imagine the front and back surfaces of the sample maintained in equilibrium with a reservoir at equilibrium, $T_{ij} = 0$. This guarantees that the macroscopic pressure drop across the sample is zero; it also guarantees the boundary condition (A 3). Therefore any poles in $\tilde{k}(\omega)$ must occur on the negative imaginary axis.

We have shown, then, that any poles or zeros in either $\tilde{\alpha}(\omega)$ or $\tilde{k}(\omega)$ must occur on the negative imaginary axis. To this point, it seems possible that there may be branch points in the lower half-plane other than on the negative imaginary axis. Let us suppose that ω^* is such a point. Let ω_1 and ω_2 be two complex frequencies on either side of the branch cut associated with ω_j^* and $\boldsymbol{u}_1(\boldsymbol{r})$ and $\boldsymbol{u}_2(\boldsymbol{r})$ be the corresponding microscopic solutions, for the same boundary conditions. The meaning of a 'branch cut' is that these two solutions are distinct. Since, in reality $\omega_1 = \omega_2$, the function $\delta\boldsymbol{u} = \boldsymbol{u}_1 - \boldsymbol{u}_2$ is a non-trivial solution to the Navier–Stokes equations, (A 1*a*), and $\delta\boldsymbol{u}$ satisfies the surface condition (A 3), because the boundary conditions on $\boldsymbol{u}_{1,2}$ cancel. The theorem proved above, however, shows that this can happen only for ω^* on the negative imaginary axis. Therefore, any branch points in $\tilde{\alpha}(\omega)$ or $\tilde{k}(\omega)$ must occur on the negative imaginary axis.

Appendix B. Finite thermal conductivity in the solid phase

In §5 we neglected the possibility that heat could flow from the He II into the solid; in this Appendix we estimate the magnitude of this neglected effect. The issue does not arise for the first sound/fourth sound mode ((5.7) in the text) because there is no temperature variation associated therewith; we have already assumed that the thermal expansion coefficient vanishes. If a finite value of the thermal expansion

coefficient is retained, Achiam & Bergman (1974) have explicitly shown that fourth sound, the low-frequency limit of (5.7), has a truly negligible attenuation due to thermal conduction into the solid. We consider, then, second sound propagating in a porous medium consisting of a periodic layering of slabs of fluid having width W_{He} and slabs of solid having width W_{Sol}. We wish to investigate the effects that the finite thermal conductivity of the solid has on the speed and attenuation of the second sound mode. Accordingly, we neglect all attenuation mechanisms in the fluid except the thermal conductivity (Putterman 1974, pp. 126 ff.), κ_{He}:

$$\rho_{\mathrm{N}} \frac{\partial \boldsymbol{u}_{\mathrm{N}}}{\partial t} = -\frac{\rho_{\mathrm{N}}}{\rho} \nabla P - \rho_{\mathrm{S}} s \nabla T, \tag{B 1a}$$

$$\rho_{\mathrm{S}} \frac{\partial \boldsymbol{u}_{\mathrm{S}}}{\partial t} = -\frac{\rho_{\mathrm{S}}}{\rho} \nabla P + \rho_{\mathrm{S}} s \nabla T, \tag{B 1b}$$

$$\nabla \cdot (\rho_{\mathrm{S}} \boldsymbol{u}_{\mathrm{S}} + \rho_{\mathrm{N}} \boldsymbol{u}_{\mathrm{N}}) + \frac{\partial (\rho_{\mathrm{N}} + \rho_{\mathrm{S}})}{\partial t} = 0, \tag{B 1c}$$

$$\nabla \cdot (\rho s \boldsymbol{u}_{\mathrm{N}}) + \frac{\partial}{\partial t} (\rho s) = \kappa_{\mathrm{He}} \nabla^2 T / T. \tag{B 1d}$$

The equation of motion in the solid is, of course, the heat equation

$$\kappa_{\mathrm{Sol}} \nabla^2 T_{\mathrm{Sol}} - C_{\mathrm{Sol}} \frac{\partial T_{\mathrm{Sol}}}{\partial t} = 0, \tag{B 2}$$

where C_{Sol} is the volumetric heat capacity. The boundary conditions at the walls are continuity of temperature,

$$T_{\mathrm{He}}|_{\mathrm{wall}} = T_{\mathrm{Sol}}|_{\mathrm{wall}}, \tag{B 3a}$$

and continuity of heat flux,

$$[T_{\mathrm{He}} \rho s \boldsymbol{u}_{\mathrm{N}} - \kappa_{\mathrm{He}} \nabla T_{\mathrm{He}}]|_{\mathrm{wall}} = -\kappa_{\mathrm{Sol}} \nabla T_{\mathrm{Sol}}|_{\mathrm{wall}}. \tag{B 3b}$$

In (B 3a) we have explicitly ignored the Kapitza resistance (Achiam & Bergman 1974); a finite value of the Kapitza resistance will act to further reduce the effects of the solid's thermal properties on the second sound mode.

It is straightforward to solve for the speed and attenuation of a mode propagating parallel to the layers. In the low-frequency limit (in which the wavelength of second sound in He II and the thermal wavelength in the solid are each larger than $W_{\mathrm{He,\,Sol}}$) the mode has a speed

$$V^2 = c_2^2 \frac{\phi C_{\mathrm{He}}}{\phi C_{\mathrm{He}} + (1-\phi) C_{\mathrm{Sol}}}, \tag{B 4a}$$

and a specific attenuation

$$\frac{1}{Q} = \frac{\omega [\phi \kappa_{\mathrm{He}} + (1+\phi) \kappa_{\mathrm{Sol}}]}{V^2 [\phi C_{\mathrm{He}} + (1-\phi) C_{\mathrm{Sol}}]}, \tag{B 4b}$$

where $\phi = W_{\mathrm{He}}/[W_{\mathrm{He}} + W_{\mathrm{Sol}}]$ is the porosity. The speed (B 4a) is only slightly altered from that of second sound in the bulk because the volumetric specific heats of solids are typically 2–3 orders of magnitude less than that of ^{4}He. The attenuation is identical in form with the relevant contribution to that of second sound in bulk ^{4}He but with a renormalized thermal conductivity and specific heat. The thermal conductivities of non-crystalline solids at these temperatures are comparable with that of ^{4}He, namely 10^{3-4} erg/(s cm K). This means that the additional attenuation of second sound due to conductivity in the solid is comparable with that in bulk ^{4}He. Specifically, for frequencies less than 10^4 Hz, the additional attenuation due to

thermal conduction in the solid is $1/Q < 10^{-3}$. Inasmuch as we are presupposing that all bulk attenuations are minor compared with that due to viscous shearing of the normal component (5.8), we are justified in neglecting this additional attenuation mechanism as well.

REFERENCES

ACHIAM, Y. & BERGMAN, D. 1974 Hydrodynamic theory of fourth sound in clamped conditions. *J. Low Temp. Phys.* **15**, 559–576.

ATTENBOROUGH, K. 1983 Acoustical characteristics of rigid fibrous absorbents and granular materials. *J. Acoust. Soc. Am.* **73**, 785–799.

AURIAULT, J.-L., BORNE, L. & CHAMBON, R. 1985 Dynamics of porous saturated media, checking of the generalized law of Darcy. *J. Acoust. Soc. Am.* **77**, 1641–1650.

AVNIR, D., FARIN, D. & PFEIFFER, P. 1984 Molecular fractal surfaces. *Nature* **308**, 261–263.

BAKER, S. 1985 Measurement of the Biot structural factor δ for sintered bronze spheres. In *Proc. IEEE Ultrasonics Symposium* (to be published).

BAKER, S. 1986 Ph.D. thesis, Dept of Physics, UCLA.

BEDFORD, A., COSTLEY, R. D. & STERN, M. 1984 On the drag and virtual mass coefficients in Biot's equations. *J. Acoust. Soc. Am.* **76**, 1804–1809.

BERGMAN, D. J. 1979 Dielectric constant of a simple cubic array of identical spheres. *J. Phys.* C: *Solid State Phys.* **12**, 4947–4960.

BERGMAN, D. J., HALPERIN, B. I. & HOHENBERG, P. C. 1975 Hydrodynamic theory of fourth sound in a moving superfluid. *Phys. Rev.* **B 11**, 4253–4263.

BIOT, M. A. 1956*a* Theory of propagation of elastic waves in a fluid-saturated porous solid. I. Low-frequency range. *J. Acoust. Soc. Am.* **28**, 168–178.

BIOT, M. A. 1956*b* Theory of propagation of elastic waves in a fluid-saturated porous solid. II. Higher frequency range, *J. Acoust. Soc. Am.* **28**, 179–191.

BIOT, M. A. 1962*a* Mechanics of deformation and acoustic propagation in porous media. *J. Appl. Phys.* **33**, 1482–1498.

BIOT, M. A. 1962*b* Generalized theory of acoustic propagation in porous dissipative media. *J. Acoust. Soc. Am.* **34**, 1254–1264.

BIOT, M. A. & WILLIS, D. G. 1957 The elastic coefficients of the theory of consolidation. *Trans. ASME* E: *J. Appl. Mech.* **24**, 594–601.

BROWN, R. J. S. 1980 Connection between formation factor for electrical resistivity and fluid–solid coupling factor in Biot's equations for acoustic waves in fluid-filled media. *Geophys.* **45**, 1269–1275.

CHANDLER, R. N. 1981 Transient streaming potential measurements on fluid-saturated porous structures: an experimental verification of Biot's slow wave in the quasi-static limit. *J. Acoust. Soc. Am.* **70**, 116–121.

CHANDLER, R. N. & JOHNSON, D. L. 1981 The equivalence of quasi-static flow in fluid-saturated porous media and Biot's slow wave in the limit of zero frequency. *J. Appl. Phys.* **52**, 3391–3395.

FROHLICH, H. 1949 *Theory of Dielectrics; Dielectric Constant and Dielectric Loss.* Clarendon.

JAYASINGHE, D. A. P., LETELIER, M. & LEUTHEUSSER, H. J. 1974 Frequency dependent friction in oscillatory laminar pipe flow. *Intl J. Mech. Sci.* **16**, 819–827.

JOHNSON, D. L. 1980 Equivalence between fourth sound and liquid He II at low temperatures and the Biot slow wave in consolidated porous media. *Appl. Phys. Lett.* **37**, 1065–1067; ibid. **38**, 827 (E).

JOHNSON, D. L. 1982 Elastodynamics of gels. *J. Chem. Phys.* **77**, 1531–1539.

JOHNSON, D. L. 1986 Recent developments in the acoustic properties of porous media. *Frontiers of Physical Acoustics, Proc. Enrico Fermi Summer School, Varenna, Italy.* Elsevier.

JOHNSON, D. L. & PLONA, T. J. 1982 Acoustic slow waves and the consolidation transition. *J. Acoust. Soc. Am.* **72**, 556–565.

JOHNSON, D. L., PLONA, T. J., SCALA, C., PASIERB, F. & KOJIMA, H. 1982 Tortuosity and acoustic slow waves. *Phys. Rev. Lett.* **49**, 1840–1844.

JOHNSON, D. L. & SEN, P. N. 1981 Multiple scattering of acoustic waves with application to the index of refraction of fourth sound. *Phys. Rev.* **B 24**, 2486–2496.

KATZ, A. J. & THOMPSON, A. H. 1985 Fractal sandstone pores: implications for conductivity and pore formation. *Phys. Rev. Lett.* **54**, 1325–1328.

KIRKPATRICK, S. 1973 Percolation and conduction. *Rev. Mod. Phys.* **45**, 574–588.

KOPLIK, J. 1981 On the effective medium theory of random linear networks. *J. Phys.* C: *Solid State Phys.* **14**, 4821–4837.

KRISS, M. 1969 Size effects in liquid helium II as measured by fourth sound and the attenuation of fourth sound. Ph.D. thesis, Department of Physics, UCLA.

LANDAU, L. D. & LIFSHITZ, E. M. 1959 *Fluid Mechanics*. Pergamon.

LANDAU, L. D. & LIFSHITZ, E. M. 1960 *Electrodynamics of Continuous Media*. Pergamon.

MANDELBROT, B. 1982 *The Fractal Geometry of Nature*. Freeman.

PINES, D. 1964 In *Elementary Excitations in Solids*, Lecture Notes and Supplements in Physics (ed. J. D. Jackson & D. Pines), p. 123 ff. Benjamin.

POLLACK, G. L. & PELLAM, J. R. 1965 Wave-mode modification in liquid helium with partially clamped normal fluid. *Phys. Rev.* **137**, A1676–A1684.

PUTTERMAN, S. J. 1974 *Superfluid Hydrodynamics*. North-Holland Elsevier.

RUDNICK, I. 1976 Physical acoustics at UCLA in the study of superfluid helium. In *New Directions in Physical Acoustics. Proc. Enrico Fermi Summer School, Course LXIII*, p. 112. Academic.

SCHEIDEGGER, A. E. 1974 *Physics of Flow Through Porous Media*. University of Toronto Press.

SHAPIRO, K. A. & RUDNICK, I. 1965 Experimental determination of the fourth sound velocity in helium II. *Phys. Rev.* **137**, A1383–A1391.

SINGER, D., PASIERB, F. RUEL, R. & KOJIMA, H. 1984 Multiple scattering of second sound in superfluid He II-filled porous medium. *Phys. Rev.* **B 30**, 2909–2912.

STOLL, R. D. 1974 Acoustic waves in saturated sediments. In *Physics of Sound in Marine Sediments* (ed. L. Hampton). Plenum.

TAM, W. Y. & AHLERS, G. 1985 Damping of fourth sound in ^{4}He due to normal fluid flow. *J. Low Temp. Phys.* **58**, 497–512.

TILLEY, D. R. & TILLEY, J. 1974 *Superfluidity and Superconductivity*. Wiley.

WEICHERT, M. & MEINHOLD-HEERLEIN, L. 1970 Theoretical studies of the propagation of sound in narrow channels filled with He II. I. The dispersion relations of fourth sound and of the fifth wave mode. *J. Low Temp. Phys.* **1**, 273.

WEICHERT, M. & PASSING, R. 1982 Observation of a new thermal wave in a planar superfluid helium layer. *Phys. Rev.* **B 26**, 6114–6122.

WONG, P.-Z., KOPLIK, J. & TOMANIC, J. 1984 *Phys. Rev.* **B 30**, 6606–6614.

ZWIKKER, C. & KOSTEN, C. W. 1949 *Sound Absorbing Materials*. Elsevier.

Note added in proof: We wish to call the readers attention to a recent article by A. N. Norris to be published in *J. Wave–Material Interactions* in which he discusses some low-frequency properties *vis-à-vis* (3.12).